8. Nonlinear Fracture Mechanics II: Crack Bridging

References:

J. W. Hutchinson, *Notes on Nonlinear Fracture Mechanics* (http://imechanica.org/node/755);
Alan Zehnder, *Lecture Notes on Fracture Mechanics* (http://hdl.handle.net/1813/3075).
G. Bao and Z. Suo, Remarks on crack-bridging concepts. *Appl. Mech. Rev.* 45, 355-366, 1992.

Dugdale-Barenblatt Model. Dugdale (*J. Appl. Mech.* 8, 100-104, 1960) observed that the plastic zone ahead of a crack tip in a thin sheet of mild steel was primarily a narrow strip of height comparable to the sheet thickness (localized plastic deformation, necking), while the length of the strip s was much longer. The elastic-plastic fracture problem is modeled by an elastic plane-stress problem with a strip of plastic zone ahead of each crack tip; the length of the plastic zone is to be determined. Assuming the material to be elastic-perfectly plastic with σ_0 as the tensile yield stress, the stress variation ahead of the crack tip is illustrated in the figure below.

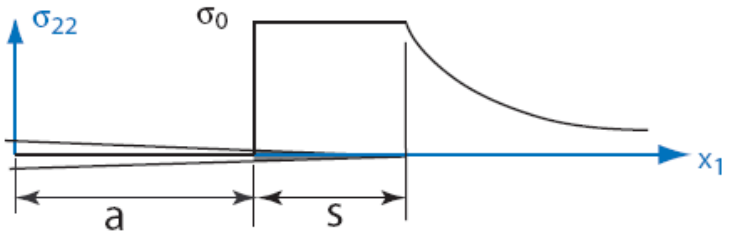

For a finite crack of length $2a$ in an infinite plate, subject to a remote tension in the direction normal to the crack plane, the plastic zone size s can be determined by considering a fictitious crack of length $2(a+s)$. In addition to the remote tension, the fictitious crack is subject to distributed normal traction over part of the crack surfaces ($a < |x| < a+s$); the plastic zone plays a role of bridging between the crack surfaces with a constant traction σ_0. The stress intensity factor at the tip of the fictitious crack ($|x| = a+L$) can be calculated by the method of linear superposition:

$$K_s = \sigma_\infty \sqrt{\pi c} - \int_a^c \frac{2}{\pi} \frac{\sigma_0 \sqrt{\pi c}}{\sqrt{c^2 - x^2}} dx$$

where the first term is due to the remote tension ($c = a + s$), and the second term is integration of the stress intensity factor due to crack face tractions (negative sign for tractions in the direction of closing the crack). Carrying out the integration, we obtain that

$$K_s = \sigma_\infty \sqrt{\pi c} - \frac{2}{\pi} \sigma_0 \sqrt{\pi c} \arccos\left(\frac{a}{c}\right).$$

However, with the presence of plastic zone, the stress is bounded at the tip with no singularity (see the figure above). This requires that $K_s = 0$ for the fictitious crack, by which the plastic zone size is determined as:

$$\frac{c}{a} = \sec\left(\frac{\pi \sigma_\infty}{2\sigma_0}\right) \text{ or } s = c - a = a\left[\sec\left(\frac{\pi \sigma_\infty}{2\sigma_0}\right) - 1\right].$$

Dugdale (1960) performed experiments with steel sheets containing center and edge cracks and measured the plastic zone lengths (by an optical method) under tension. The agreement between the experiments and the above model was excellent (see figure).

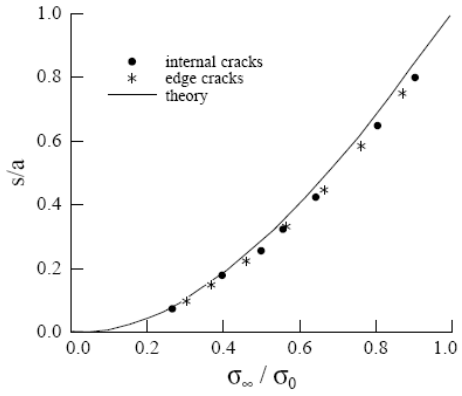

The plastic deformation ahead of the crack tip leads to an opening displacement at the original crack tip ($|x| = a$). Again, by the method of linear superposition, the crack-tip opening displacement (CTOD) is obtained as

$$\delta_t = \frac{4\sigma_\infty}{E}\sqrt{c^2 - a^2} - \frac{8\sigma_0}{\pi E}\left[\sqrt{c^2 - a^2}\arccos\left(\frac{a}{c}\right) - a\ln\left(\frac{c}{a}\right)\right]$$

With the previously determined plastic zone size s, the CTOD becomes

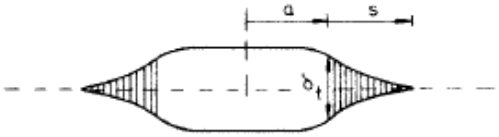

$$\delta_t = a\frac{8\sigma_0}{\pi E}\ln\left(\sec\left(\frac{\pi\sigma_\infty}{2\sigma_0}\right)\right)$$

Next we develop the condition for initiation of crack growth. The plastic zone may also be regarded as a bridging zone with a traction-displacement relationship. The assumption of perfectly plasticity leads to a constant traction within the plastic bridging zone. The bridging however is broken when the opening displacement reaches a critical level (δ_c). Thus, the initiation of crack growth is predicted when $\delta_t = \delta_c$.

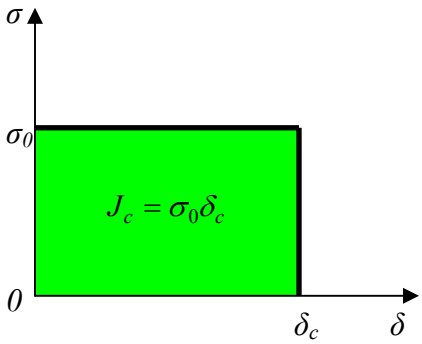

It was shown that the J-integral around the crack tip is related to the CTOD as:

$$J = \sigma_0\delta_t$$

Thus, an equivalent condition for fracture initiation may be stated in terms of a critical energy release rate (or fracture energy), $J_c = \sigma_0\delta_c$, which corresponds to the area under the traction-displacement curve for crack bridging (see figure). The critical opening displacement δ_c or the critical energy release rate J_c may be experimentally determined using appropriate test specimen.

Using the above determined CTOD, the critical remote stress for fracture initiation is determined:

$$\sigma_c = \frac{2}{\pi}\sigma_0\arccos\left[\exp\left(-\frac{\pi E\delta_c}{8\sigma_0 a}\right)\right]$$

Small-scale yielding or large-scale yielding. It is instructive to compare the Dugdale-Barenblatt model with LEFM to further understand the condition of small scale yielding. When $\sigma_\infty / \sigma_0 << 1$, the results from the Dugdale-Barenblatt model reduce to

$$s = a\left[\sec\left(\frac{\pi\sigma_\infty}{2\sigma_0}\right) - 1\right] = a\left[\frac{\pi^2}{8}\frac{\sigma_\infty^2}{\sigma_0^2} + O\left(\frac{\sigma_\infty^4}{\sigma_0^4}\right)\right]$$

$$\delta_t = a\frac{8\sigma_0}{\pi E}\ln\left(\sec\left(\frac{\pi\sigma_\infty}{2\sigma_0}\right)\right) = a\left[\frac{\pi\sigma_\infty^2}{E\sigma_0} + O\left(\frac{\sigma_\infty^4}{\sigma_0^4}\right)\right]$$

$$J = \sigma_0\delta_t \approx \frac{\pi\sigma_\infty^2 a}{E}$$

Recall that $K = \sigma_\infty\sqrt{\pi a}$ and $J = G = \frac{K^2}{E}$ in LEFM under the SSY condition. The energy release rate from LEFM agrees closely with the J-integral from the Dugdale-Barenblatt model for remote stresses up to approximately $\sigma_\infty / \sigma_0 = 0.4$. The corresponding plastic zone size is up to $s/a \approx 0.2$. Thus the SSY condition is valid when the plastic zone size is less than 20% of the crack length.

The critical stress for fracture initiation predicted by the Dugdale-Barenblatt model extends the previous prediction by LEFM from small scale yielding to large scale yielding. Substituting the critical stress into the solution for the plastic zone size (set $\sigma_\infty = \sigma_c$), we obtain the critical plastic zone size

$$s_c = a\left[\exp\left(\frac{\pi E\delta_c}{8\sigma_0 a}\right) - 1\right]$$

The small scale yielding condition requires that $s_c / a << 1$, and thus $\frac{\pi E\delta_c}{8\sigma_0 a} << 1$ or $a >> \frac{\pi E\delta_c}{8\sigma_0}$.

An intrinsic length scale emerges: $L = \frac{\pi E\delta_c}{8\sigma_0}$, which depends on the material properties only. Only when the crack size is large compare to *L*, LEFM is applicable. An order-of-magnitude estimate of the length scale gives *L* ~ 1 mm for steel and *L* ~ 10 nm for ceramics.

Rewrite the critical stress in terms of the critical plastic zone size:

$$\sigma_c = \frac{2}{\pi}\sigma_0 \arccos\left[\frac{1}{1 + s_c / a}\right]$$

Therefore, under SSY condition ($s_c / a << 1$), the critical stress reduces to

$$\sigma_c \approx \frac{2}{\pi}\sigma_0\sqrt{\frac{2s_c}{a}} \approx \sqrt{\frac{E\sigma_0\delta_c}{\pi a}}$$

which agrees with the LEFM condition, $\sigma_c = \frac{K_c}{\sqrt{\pi a}}$, with $K_c = \sqrt{EJ_c} = \sqrt{E\sigma_0\delta_c}$. On the other hand, when $s_c / a >> 1$, we have $\sigma_c \approx \sigma_0$, corresponding to the global yielding condition. Therefore, the Dugdale-Barenblatt model successfully captured both linear elastic fracture mechanics (small scale yielding) and nonlinear elastic-plastic fracture mechanics (large scale

yielding) regimes, with limitations in the assumptions of perfectly plastic deformation (no hardening) and highly localized plastic zone (a narrow strip).

Generalized crack bridging concept-cohesive zone model. Barenblatt (1962) generalized the plastic strip model to a cohesive zone model in which the stress in the cohesive zone ahead of the crack is a function of the displacement rather than a constant yield stress. Cottrell (1963) put forward the concept of crack bridging as a unifying theory for fracture at various length scales, from atomic bond breaking in monolithic ceramics to fiber pull-out in composite materials. In each case, the microscopic mechanism of fracture and associated inelastic processes are represented by a bridging law that relates the face tractions in the bridging zone (or cohesive zone) to the relative displacements. The essential features of crack bridging were reviewed by Bao and Suo (1992), emphasizing their implications for strength and fracture resistance of ceramic matrix composites. The concept has also been widely used for modeling interfaces between elastic and/or elastic-plastic materials (see a review by *Hutchinson and Evans, Acta Mater. 48, 125-135, 2000*).

Unlike LEFM where the microscopic mechanisms of fracture are essentially ignored (all material aspects are lumped into one parameter, *fracture toughness*), the bridging law or the traction-displacement relation in the cohesive zone model depends on the material and the associated fracture mechanism. For example, in an ideally brittle material, fracture occurs by atomic bond breaking, for which a bridging law may be derived from an interatomic bond potential. To be specific, consider an empirical potential for a covalent bond in form of

$$U = -\frac{A}{r^m} + \frac{B}{r^n} \quad (m < n)$$

where r is the separation between two atoms. The interatomic force as a function of the separation is

$$F = \frac{dU}{dr} = \frac{mA}{r^{m+1}} - \frac{nB}{r^{n+1}}$$

where the first term represents an attractive force (positive) and second term represents a repulsive force (negative). By setting $F = 0$, the equilibrium separation between the two atoms can be determined:

$$r_0 = \left(\frac{nB}{mA}\right)^{\frac{1}{n-m}}$$

For two solid blocks held together by such atomic bonds (see figure), the stress as the total force per unit area is related to the separation between two planes within the material:

$$\sigma = NF = \frac{1}{r_0^2}\left(\frac{mA}{r^{m+1}} - \frac{nB}{r^{n+1}}\right)$$

where $N = 1/r_0^2$ is the number of atomic bonds per unit area. Rewrite the stress as a function of the displacement from the equilibrium separation, $\delta = r - r_0$:

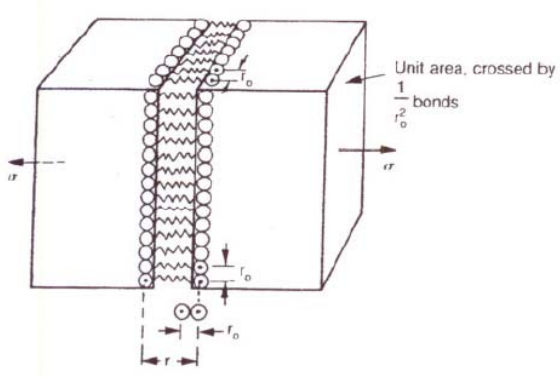

$$\sigma(\delta) = \alpha\sigma_0\left[\left(\frac{r_0}{r_0+\delta}\right)^{m+1} - \left(\frac{r_0}{r_0+\delta}\right)^{n+1}\right]$$

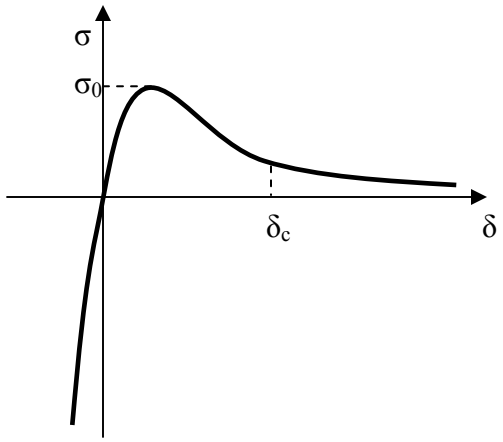

where σ_0 is the maximum stress and α is a prefactor of order unity (depending on the exponents *n* and *m*). A sketch of this traction-displacement relation is shown below. The maximum stress σ_0 can be related to the elastic modulus of the material:

$$\sigma_0 = \frac{E}{\alpha(n-m)}$$

σ_0 is roughly one order of magnitude lower than the modulus (e.g., $E \sim 10^{11}$ N/m^2 and $\sigma_0 \sim 10^{10}$ N/m^2). A cut-off separation (r_c) between the atoms is often specified for the empirical potential, beyond which the atomic bond is regarded as broken and thus no interaction between the atoms ($F = 0$). The critical displacement, $\delta_c = r_c - r_0$ is typically comparable to the equilibrium separation r_0 (in the order of 10^{-10} m). In addition to tensile stresses ($\sigma > 0$) typically expected for crack bridging with $\delta > 0$, a compressive stress (repulsion) occurs when $\delta < 0$, which may be important for cases with contacts between the crack surfaces (e.g., under mixed mode loading).

With the above traction-displacement relation as the bridging law for the ideally brittle material, the fracture energy per unit area is

$$\Gamma = \int_0^{\delta_c} \sigma d\delta \sim \sigma_0\delta_c$$

An order-of-magnitude estimate gives that $\Gamma \sim 1$ J/m^2, which is essentially the surface energy per unit area of the solid. Therefore, the bridging law based on the atomic bond breaking mechanism effectively predicts the fracture energy of ideally brittle materials.

For metals, however, the fracture mechanism is different, with large plastic deformation (local necking) and void nucleation, growth, and coalescence ahead of the crack tip. The bridging law, $\sigma(\delta)$, may be derived from detailed micromechanics models or may be determined experimentally (Cox, 1991). Relatively simple bridging laws are often used in theoretical and numerical analyses. For example, the Dugdale model assumes a constant traction in the bridging zone. A triangular or trapezoidal shaped traction-displacement curve is frequently used in practice. In any case, the maximum stress σ_0 and the critical displacement δ_c are the two most important parameters. For ductile fracture, σ_0 corresponds to the yield stress (~10^8 N/m^2), and δ_c is typically in the order of 10^{-6} m (depending on the microstructures). The fracture energy of metals is thus much higher than the surface energy: $\Gamma \sim 10^2$ J/m^2.

Bridging laws have also been developed for adhesion and debonding of interfaces between two dissimilar materials (Hutchinson and Evans, 2000); the constituent materials can be either linear elastic or elastic-plastic. Depending on the material systems, the maximum stress of the bridging law σ_0 can be either small or large compared to the yield stress of the constituent material. When σ_0 is greater than the yield stress, plastic deformation in the constituent material

occurs during interfacial fracture, and the total energy of fracture is greater than the intrinsic fracture energy Γ ($\sim \sigma_0 \delta_c$). The effect of plasticity can be analyzed by coupling the bridging law for the interface with continuum elastic-plastic models for the constituent materials. A few examples were reviewed by Hutchinson and Evans (2000).

A simple bridging law for adhesive interactions between two solid surfaces can be derived from the classical Lennard-Jones potential (Springman and Bassani, JMPS, 2008):

$$\sigma(\delta) = \frac{3\sqrt{3}}{2}\sigma_0 \left[\left(\frac{r_0}{r_0 + \delta} \right)^3 - \left(\frac{r_0}{r_0 + \delta} \right)^9 \right]$$

Similar to the covalent bond bridging, r_0 is the equilibrium separation. However, the adhesive interaction is typically weaker ($\sigma_0 \sim 10^7$ N/m^2), but with a longer range (cut-off displacement $\delta_c \sim 10 r_0 \sim 10^{-8}$ m). The adhesion energy is thus relatively low: $\Gamma \sim 0.1$ J/m^2. A large portion of the interfacial fracture energy measured from experiments may be due to extrinsic plastic deformation of constituent materials.

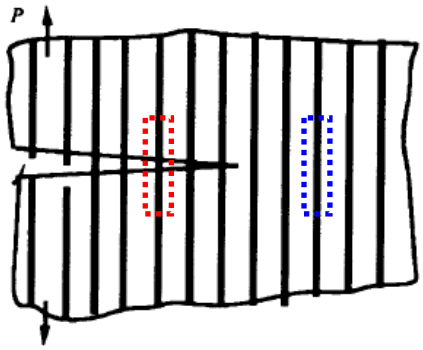

Crack bridging in ceramic composites (Bao and Suo, 1992). As an example of the applications of the crack bridging concept, we consider fiber-reinforced ceramic matrix composites. Ceramics are brittle and prone to fracture. Strong fibers in ceramic matrix can enhance the resistance to fracture; the diameter of the fiber is typically in the range of 1 – 100 μm. As a crack front reaches a fiber, the fiber is pulled out from the matrix with interfacial sliding; additional energy is dissipated by friction. As the crack front advances, some fibers remain intact, bridging the crack surfaces. A bridging law was developed by a simple model described as follows.

First consider a reference state with parallel fibers in an elastic matrix subjected to an average axial stress $\bar{\sigma}$. By a simple rule of mixture, the effective modulus of the composite is

$$\bar{E} = fE_f + (1-f)E_m$$

where E_f and E_m are Young's modulus of the fiber and the matrix, respectively, and f is the volume fraction of the fiber in the composite. The axial strain of the composite is then

$$\bar{\varepsilon} = \frac{\bar{\sigma}}{\bar{E}}$$

With no cracking or sliding, the axial strains in the fiber and the matrix are identical, $\varepsilon_f = \varepsilon_m = \bar{\varepsilon}$. Thus the stresses in the fiber and the matrix are, respectively

$$\sigma_f = \frac{E_f}{\bar{E}}\bar{\sigma} \text{ and } \sigma_m = \frac{E_m}{\bar{E}}\bar{\sigma}$$

Next, consider the region where the matrix is fractured and bridged by the continuous fibers. The bridging fibers are pulled out as the crack surfaces open. Sliding at the fiber/matrix interface occurs over a length s on both sides of the crack; s is to be determined. The stress in the fiber now is redistributed with a variation along the axial direction. Assume a constant friction

force per unit area, τ, along the sliding interface, and assume s to be large compared to the fiber radius R ($s >> R$). By a shear lag model, the equilibrium of the fiber requires that

$$\frac{d\sigma_f}{dz} = -\frac{2\tau}{R}$$

The boundary conditions are: (i) At $z = 0$, the matrix has fractured and all the applied load is carried by the fiber, thus, $\sigma_f = \frac{\bar{\sigma}}{f}$. (ii) At $z = s$, the fiber is perfectly bonded to the matrix with no sliding, thus $\sigma_f = \frac{E_f}{\bar{E}}\bar{\sigma}$ (the reference state). Solving the differential equation with the boundary conditions, we obtain that, for $|z| < s$

$$\sigma_f(z) = \frac{\bar{\sigma}}{f} - \frac{2\tau}{R}z$$

and the sliding length

$$s = \frac{R\bar{\sigma}}{2\tau}\left(\frac{1}{f} - \frac{E_f}{\bar{E}}\right)$$

The axial strain of the fiber is

$$\varepsilon_f(z) = \frac{\bar{\sigma}}{fE_f} - \frac{2\tau}{E_f R}z$$

The relative opening displacement between the two planes at $z = \pm s$ is

$$\delta_2 = 2\int_0^s \varepsilon_f(z)dz = \frac{2\bar{\sigma}s}{fE_f} - \frac{2\tau s^2}{E_f R}$$

Subtracting the elastic displacement at the reference state ($\delta_1 = 2\bar{\varepsilon}s$) from the total displacement, we obtain the separation displacement of the crack faces:

$$\delta = \delta_2 - \delta_1 = \frac{2\bar{\sigma}s}{fE_f} - \frac{2\tau s^2}{E_f R} - \frac{2\bar{\sigma}s}{\bar{E}}$$

Reorganizing the above result gives a bridging law:

$$\bar{\sigma}(\delta) = \frac{f\bar{E}}{(1-f)E_m}\sqrt{\frac{2E_f\tau\delta}{R}}$$

Take the strength of the fiber as S_f (which may depend on the fiber radius), the critical average stress is then $\sigma_0 = fS_f$ (when the fiber breaks). By the bridging law, the corresponding opening displacement is

$$\delta_c = \frac{(1-f)^2 E_m^2 S_f^2}{2E_f\bar{E}^2\tau}R$$

The bridging law can then be rewritten as

$$\bar{\sigma}(\delta) = \sigma_0\sqrt{\frac{\delta}{\delta_c}}$$

Typically, $S_f \sim 10^9$ N/m^2, $\tau \sim 10^7$ N/m^2, and thus $\sigma_0 = fS_f \sim 10^8$ N/m^2, $\delta_c \sim R \sim 10^{-5}$ m. The fracture energy for the composite is then $\Gamma \sim \sigma_0\delta_c \sim 10^3$ J/m^2, much greater than the fracture

energy for the ceramic matrix (~1 J/m^2). Therefore, the fiber reinforcement with the pull-out bridging mechanism greatly enhances the fracture resistance for the composite. It is noted that the fracture energy is very sensitive to the fiber strength, $\Gamma \sim S_f^3$. Increasing the fiber strength (e.g., by reducing the fiber radius) can significantly improve the fracture resistance of the ceramic composite. It may also be interesting to note that, based on this bridging model, the ceramic composite has the best fracture resistance with a fiber volume fraction, $f = 1/3$.

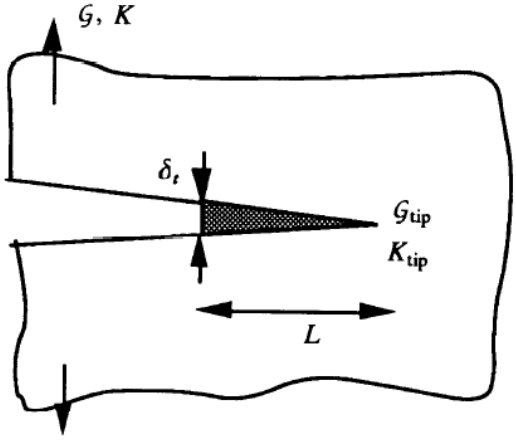

Small-scale bridging. The size of the bridging zone ahead of the crack tip may be estimated under the condition of small scale bridging (similar to the SSY condition for elastic-plastic fracture). Assume that the bridging zone size is small compared to the crack size, $L << a$. In this case, the external load can be represented by the stress intensity factor K or energy release rate G, ignoring the details of the bridging zone. The crack starts to grow in the matrix when $G = \Gamma_0$, where Γ_0 is the fracture energy of the ceramic matrix. As the crack front advances, a fiber bridging zone develops (see figure). An application of J-integral along a contour at the boundary of the bridging zone gives that

$$G = J = G_{tip} + \int_0^{\delta_t} \bar{\sigma}(\delta) d\delta$$

While fracture of the matrix at the tip of the bridging zone still occurs with $G_{tip} = \Gamma_0$, the energy dissipation by friction to pull out the fibers requires increasing energy release rate, depending on the bridging law, $\bar{\sigma}(\delta)$.

The size of the bridging zone L increases as the applied load (G) increases, until a steady state is reached when the fibers at the end of the bridging zone start to break ($\delta_t = \delta_c$). Subsequently, the bridging zone size remains a constant $L = L_{SS}$ as the crack grows. The required energy release for the steady state growth is:

$$\Gamma_{SS} = \Gamma_0 + \int_0^{\delta_c} \bar{\sigma}(\delta) d\delta$$

To determine the resistance curve (R-curve) and the steady state bridging zone size, a boundary value problem has to be solved. Within the bridging zone, the face traction is related to the opening displacement by the bridging law. The outer boundary condition is given by the K field corresponding to the applied energy release rate G. Given a bridging zone size L, the stress intensity factor at the crack tip can be calculated by linear superposition (LEFM):

$$K_{tip} = K - K_{bridging}(L)$$

The opening displacement at the end of the bridging zone can be calculated in a similar manner:

$$\delta_t = \delta_{t1}(K, L) - \delta_{t2}(L)$$

A dimensional analysis leads to the following:

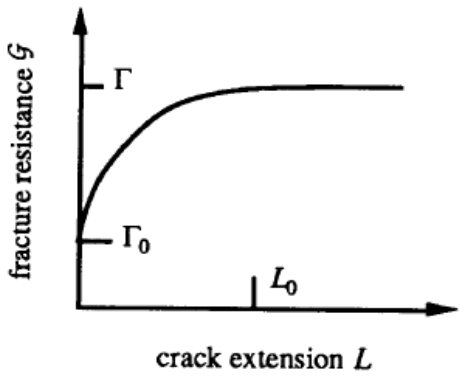

$$\frac{K_{tip}}{\sigma_0\sqrt{L}} = f\left(\frac{K}{\sigma_0\sqrt{L}}, \frac{\sigma_0 L}{E\delta_0}\right) \text{ and } \frac{\delta_t}{\delta_c} = g\left(\frac{K}{\sigma_0\sqrt{L}}, \frac{\sigma_0 L}{E\delta_0}\right)$$

The functions f and g will also depend on the shape of the bridging law. Note that Irwin's relation holds at both the local and the global levels: $G = \frac{K^2}{E'}$ and $G_{tip} = \frac{K_{tip}^2}{E'}$.

Setting $K_{tip} = K_0 = \sqrt{E'\Gamma_0}$, we obtain the R curve: $K = K(L)$ or $G = G(L)$:

$$f\left(\frac{K}{\sigma_0\sqrt{L}}, \frac{\sigma_0 L}{E\delta_0}\right) = \sqrt{\frac{E'\Gamma_0}{\sigma_0^2 L}}$$

Setting $\delta_t = \delta_c$ with $K = K(L)$, we obtain the steady state bridging zone size by the equation:

$$g\left(\frac{K(L_{SS})}{\sigma_0\sqrt{L_{SS}}}, \frac{\sigma_0 L_{SS}}{E\delta_0}\right) = 1$$

It may be confirmed that at $K(L_{SS}) = \sqrt{E'\Gamma_{SS}}$.

As a simple example, consider a rectilinear bridging law: $\sigma(\delta) = \sigma_0$ for $0 < \delta < \delta_c$ and $\sigma(\delta) = 0$ for $\delta > \delta_c$. In this case, we have

$$K_{tip} = K - 2\sigma_0\sqrt{\frac{2L}{\pi}}$$

Therefore, the R curve is

$$K(L) = K_0 + 2\sigma_0\sqrt{\frac{2L}{\pi}}$$

The steady state fracture energy, $\Gamma_{SS} = \Gamma_0 + \sigma_0\delta_c$. Setting $K(L_{SS}) = \sqrt{E'\Gamma_{SS}}$, we obtain that

$$L_{SS} = \frac{\pi E'\delta_c}{8\sigma_0}\left[\sqrt{1+\frac{\Gamma_0}{\sigma_0\delta_c}} - \sqrt{\frac{\Gamma_0}{\sigma_0\delta_c}}\right]^2 \sim \frac{E'\delta_c}{\sigma_0}$$

The small scale bridging condition is satisfied when the crack size $a >> L_{SS}$.

Large-scale bridging. The small scale bridging condition is rarely satisfied in practice for composites. When large scale bridging occurs, the R curve depends sensitively on the specimen geometry and thus cannot be used to predict the strength and load carrying capacity of components of different sizes and geometry. A full stress analysis coupling the specimen geometry and the bridging law must be carried out to predict the mechanical properties including the resistance to fracture.

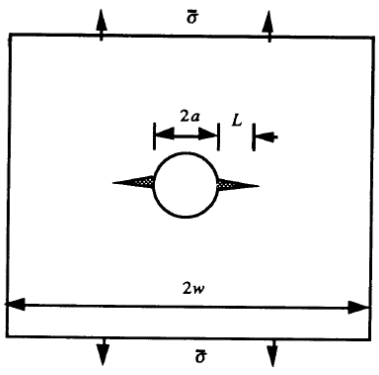

As an example, consider a panel with a circular hole. The maximum load the panel can carry depends on the material of the panel as well as the relative hole size *a*/*w*. For a monolithic ceramic panel, the maximum load is such that the

stress at the hole is below the strength of the ceramics, σ_0, which depends on the flaw size ($\sigma_0 \sim K_c/\sqrt{c}$). The stress concentration factor C is a function of a/w, and $C = 3$ for $a/w \to 0$. Therefore, the ceramic panel is brittle and notch sensitive (even a small hole reduces the load carrying capacity of the panel), with the maximum permissible stress:

$$\bar{\sigma}_{\max} = \frac{\sigma_0}{C}$$

For a ductile metal panel, plasticity relieves stress concentration near the hole and makes the panel notch insensitive. The maximum permissible load depends on the yield stress of the metal, roughly

$$\bar{\sigma}_{\max} = \sigma_0\left(1 - \frac{a}{w}\right)$$

Small holes ($a/w \to 0$) do not reduce much of the load carrying capacity for metal panels.

For a fiber-reinforced ceramic panel, matrix cracking with fiber-bridging near the hole provides a mechanism for ductile-brittle transition (see figure). When $a >> \frac{E'\delta_c}{\sigma_0}$, the small scale bridging condition is satisfied, and the panel is ceramic-like brittle. For a large panel ($a/w \to 0$), the maximum load $\bar{\sigma}_{\max} \sim \frac{\sigma_0}{3}$. When $a << \frac{E'\delta_c}{\sigma_0}$, large scale bridging prevails, and the panel is metal-like ductile. The maximum load, $\bar{\sigma}_{\max} \sim \sigma_0$. Therefore, the load carrying capacity of the panel depends on both the hole size and the bridging law.

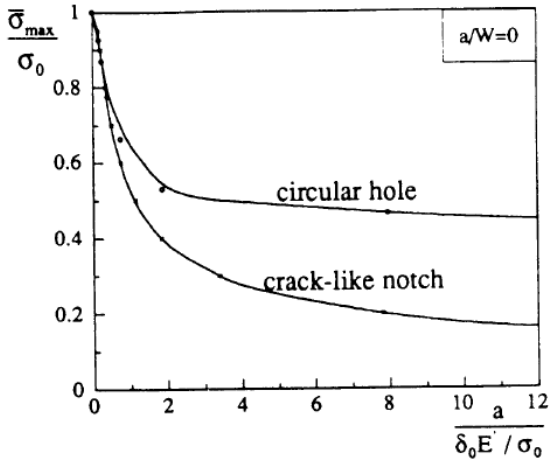

To conclude the discussions on crack bridging, we list the representative properties for different bridging mechanisms in the table below. It should be emphasized that, as a unifying concept for fracture (linear or nonlinear), crack bridging couples mechanics and materials through specific fracture/bridging mechanisms. While all the bridging mechanisms can be represented by traction-displacement relations, the large variation in the bridging scales (σ_0 and δ_c) underlies the richness in the fracture behavior of materials.

Bridging mechanism	Example material	Strength, σ_0 (N/m^2)	Critical displacement, δ_c (m)	$\Gamma \sim \sigma_0\delta_c$ (J/m^2)	$L \sim E\delta_c/\sigma_0$ (m)
Atomic bond	ceramics	10^{10}	10^{-10}	1	10^{-9}
Plastic zone	metals	10^{8}	10^{-6}	10^{2}	10^{-3}
Adhesive interactions	bimaterial interfaces	10^{7}	10^{-8}	0.1	10^{-4}
Fiber bridging	Ceramic composites	10^{8}	10^{-5}	10^{3}	10^{-2}